forests

MDPI

Article

Unraveling the Environmental and Physiological Controls on Yield and Quality of *Epimedium pubescens* Through a Shading Gradient Experiment in Agroforestry Systems

Doudou Li †, Hongbiao Zhang †, Dingmei Wen, Fengmei Suo and Baolin Guo *

State Key Laboratory for Quality Ensurance and Sustainable Use of Dao-di Herbs, Institute of Medicinal Plant Development, Chinese Academy of Medical Sciences & Peking Union Medical College, Beijing 100193, China; missbean92@163.com (D.L.); 13355386684@163.com (H.Z.); 13507004781@163.com (D.W.); fmsuo@implad.ac.cn (F.S.)

* Correspondence: blguo@implad.ac.cn

† These authors contribute equally to this work.

Abstract

Epimedium pubescens, a shade-tolerant medicinal plant, currently faces supply shortages. To investigate the regulatory mechanisms of shading intensity on its growth and quality, this study established four treatments under a *Phoebe zhennan* plantation: inter-row artificial shading (0% shading, S-0; 50% shading, S-50; 75% shading, S-75) and natural canopy shading (S-93). When monitoring environmental factors, photosynthetic parameters, biomass, and total flavonol glycoside content, significant differences among treatments were only observed regarding solar radiation. Compared with inter-row treatments, S-93 reduced the maximum net photosynthetic rate and per-plant biomass by 33%–86% and 35%–71%, respectively. Structural equation modeling revealed that understory radiation indirectly influenced yield by regulating the vapor pressure deficit and net photosynthetic rate (R^2 = 0.95). Economic assessments, based on hectare-scaled yield (converted from plot units) and input costs (seedlings, land rental, labor), indicated that the 75% inter-row shading treatment applied from July to October (S-75) was optimal, generating a net annual income of 56,924.5 USD·ha^{-1}. This study provides a theoretical basis for the understory cultivation of *E. pubescens*.

Keywords: *Epimedium pubescens*; shading intensity; photosynthetic parameters; biomass; total flavonoid glycosides

Check for updates

Academic Editor: Ilona Mészáros

Received: 27 January 2026
Revised: 25 February 2026
Accepted: 3 March 2026
Published: 4 March 2026

Copyright: © 2026 by the authors. Licensee MDPI, Basel, Switzerland. This article is an open access article distributed under the terms and conditions of the Creative Commons Attribution (CC BY) license.

1. Introduction

China has a long history of agroforestry, a practice that enhances both land-use efficiency and agricultural sustainability [1–6]. *Phoebe zhennan* S. Lee, a valuable timber species widely cultivated in southern China, is highly prized for its wood quality [7–10]. However, its long growth cycle creates a significant economic gap before timber harvest. To bridge this gap and address the growing scarcity of arable land, developing the understory economy has become a crucial strategy. This involves introducing shade-tolerant cash crops into *P. zhennan* stands to generate early returns and maximize land use.

Epimedium pubescens Maxim., a shade-preferring medicinal plant, is an ideal candidate for such understory cultivation. Highly sought after for its pharmacological properties—notably in treating osteoporosis—its market demand far exceeds current supply, which is constrained by the limited amount of arable land [11–14]. While understory agroforestry

is a promising solution to boost production, the optimal light conditions for cultivating *E. pubescens* under *P. zhennan* canopies, and how these conditions affect its growth and quality, remain unclear [15]. This knowledge gap hinders the optimization of this sustainable production model. Therefore, this study aims to investigate the growth and physiological responses of *E. pubescens* to different understory light environments.

Light is a critical environmental factor, profoundly influencing the productivity and quality of understory crops in agroforestry systems [16,17]. Extensive research shows that the understory light environment dually regulates plant growth. Severe shading can inhibit growth and reduce yields; for example, yield reductions of 14.1%–66.9% have been reported in systems such as apricot–cotton [18] and tree–peony [19]. Conversely, suitable light levels can enhance the yield of medicinal plants like *Polygonatum cyrtonema* by 9.3%–36.76% [20]. Consequently, the optimal regulation of the light environment is essential for maximizing productivity and economic benefits in agroforestry systems. Light availability also significantly affects secondary metabolism. While shading reduced both yield and active ingredients in *Desmodium styracifolium* [21], full sunlight increased flavonoid and saponin accumulation in *Gynostemma pentaphyllum*, despite inhibiting growth [22]. Notably, understory environmental factors are interconnected and interact synergistically [23]. Changes in light inevitably alter air temperature and humidity, which may further affect crop performance. For instance, understory temperature significantly influences the quality of *Panax ginseng* [24], while air humidity is a key factor for *E. pubescens* yield [15]. Given this complex interplay, a critical question remains: how do the yield and quality of *E. pubescens*, cultivated under widely spaced *P. zhennan* plantations, respond to these integrated environmental factors? Therefore, we propose the first hypothesis of this study: the heterogeneous understory light environment leads to differential patterns of yield and quality accumulation in *E. pubescens*, with specific shading intensities potentially optimizing the trade-off between biomass production and secondary metabolite synthesis.

Photosynthesis, the fundamental physiological process governing plant biomass accumulation [25–27], is highly responsive to environmental fluctuations [28]. Previous research has demonstrated that photosynthetic traits (e.g., net photosynthetic rate) in *E. pubescens* not only exhibit significant sensitivity to light intensity but also directly regulate biomass accumulation and secondary metabolite synthesis by modulating photosynthetic carbon assimilation efficiency [29–34]. In the walnut–*Polygonatum kingianum* agroforestry system, photosynthetic parameters accounted for 90.2% of the variation in *P. kingianum* yield, with the net photosynthetic rate making the greatest direct contribution [3]. Studies focusing on *Panax quinquefolius* revealed a positive correlation between morphological traits (plant height, leaf length) and photosynthetic performance (net photosynthetic rate, transpiration rate), but a negative association between ginsenoside content and photosynthetic rate [35]. Furthermore, Ma et al. [32] demonstrated that light intensity synchronously optimizes both the yield and quality of *E. pubescens* by regulating carbon partitioning in photosynthesis. However, the studies were conducted exclusively under indoor potted conditions, where the environment is relatively homogeneous and cannot systematically reflect the complex variations in actual field conditions. Therefore, there is an urgent need to conduct gradient light environment research under real field conditions to enhance the practical applicability of the findings. So, we further hypothesized that the net photosynthetic rate of *E. pubescens* leaves, as the primary physiological integrator of light micro-environmental variation, serves as the core determinant driving spatial differences in biomass accumulation and ultimate yield under contrasting understory positions.

In this study, gradient shading treatments were applied under a widely spaced *P. zhennan* plantation to create distinct understory microenvironments. By combining in situ measurements of environmental factors and physiological indicators with periodic

sampling to assess the yield and quality of *E. pubescens*, we investigated the characteristics and mechanisms underlying the effects of these microenvironments on the plant's productivity and medicinal properties. The study aims to elucidate (1) the dynamic changes in understory microenvironments and the photosynthetic characteristics of *E. pubescens* under these conditions; (2) the variations in yield and quality of *E. pubescens* across different microenvironments; and (3) the environmental and physiological mechanisms influencing yield and quality formation of *E. pubescens* cultivated under *P. zhennan*. The findings will provide a theoretical basis for microenvironment selection in the understory cultivation of shade-tolerant medicinal plants and offer precise management strategies for the standardized understory production of *E. pubescens*.

2. Materials and Methods

2.1. Description of the Study Area

The study was carried out in Shawan District (29°11′–29°31′ N, 103°25′–103°44′ E), Leshan City, Sichuan Province, China. The region has a northern subtropical mountain monsoon climate, with an average annual temperature of 18.8 °C, a precipitation of 1111 mm, a relative humidity of 79.8%, and 1091.6 annual sunshine hours (representing a 23% sunshine rate). The frost-free period averages 330 days per year. Shawan District is the largest cultivation base for *E. pubescens* in China, with a planting area of 333 hectares, and has been designated "The Hometown of Chinese *E. pubescens*".

2.2. Field Experiments Design

The study was conducted in an *Epimedium pubescens* industrial park under a *Phoebe zhennan* plantation in Shawan District, Leshan City, Sichuan Province, China. The experimental site featured flat terrain with no slope variation. The *P. zhennan* trees were planted in 2019 with a spacing of 2 m × 7 m, and exhibited consistent age, tree height, and crown diameter, providing homogeneous understory light conditions and soil background values, which established favorable baseline conditions for the field experiment.

Given the relatively small crown diameter of *P. zhennan* (approximately 2 m) and the wide row spacing (7 m), the natural shading provided by this wide-row planting pattern was insufficient to meet the optimal growth requirements of shade-tolerant species such as *E. pubescens*. Therefore, artificial shading treatments were necessary to optimize the growing environment.

Although the environmental conditions of the experimental site were relatively uniform, a randomized complete block design was employed to control for potential minor soil heterogeneity. Three blocks were established along the direction of tree rows. Three artificial shading treatments were applied, no shading net (S-0), 50% shading (S-50), and 75% shading (S-75), where the conventional 75% shading served as the upper limit for the shading gradient selection between the *P. zhennan* rows. Each treatment was replicated three times, resulting in a total of nine experimental plots. Each plot measured 16 m in length and 7 m in width, with an area of 112 m^2. Within each plot, *E. pubescens* was planted in five ridges (80 cm wide × 20 cm high). Among these five ridges, the three middle ridges were subjected to artificial shading treatments, while the two ridges adjacent to the trees were under natural canopy shading. Each ridge contained three rows of *E. pubescens* planted at a spacing of 0.3 m × 0.3 m (Figure 1). Additionally, the two outermost rows in each plot were designated as border rows to eliminate edge effects.

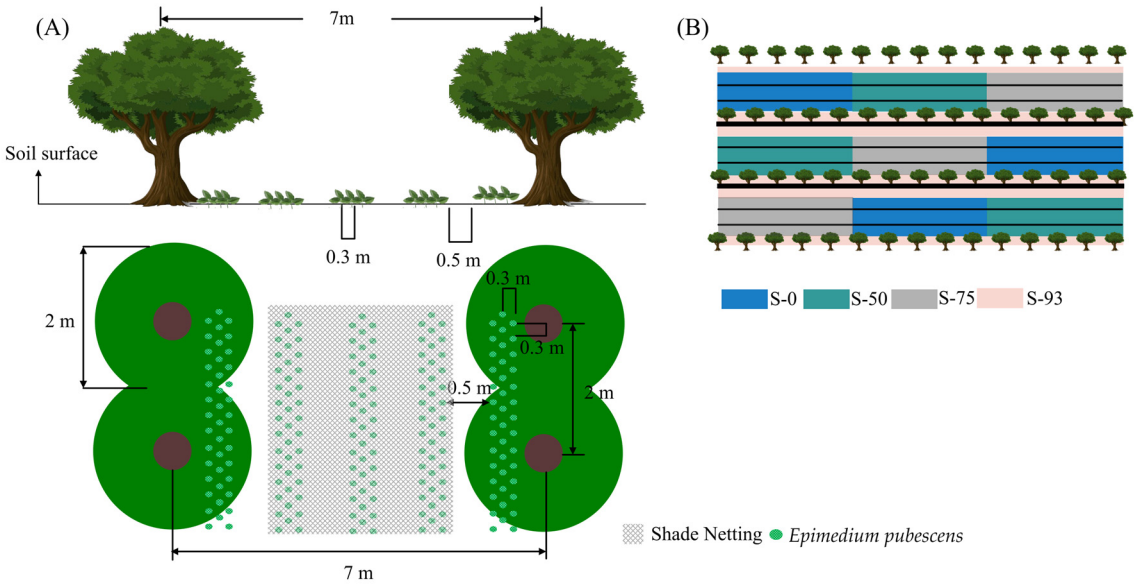


Figure 1. Planting layout and completely randomized block experimental design of *Epimedium pubescens* under different experimental treatments. (**A**) Planting layout of *E. pubescens* in intercropping system. (**B**) Completely randomized block experimental design of *E. pubescens* in intercropping system. S-0, S-50, S-75 and S-93 represent 0% shading, 50% shading, 75% shading and 93% shading (under canopy), respectively.

The shading nets used in this experiment were purchased from Greenland Shading Co., Ltd. (Taizhou, Zhejiang, China). Two shading gradients were established by covering areas with nets featuring nominal shading rates of 50% and 75%, respectively, as specified by the manufacturer. The nets were made of polyethylene (PE) incorporating 0.5% ultraviolet stabilizer (UV) to ensure anti-aging properties. During the experimental period, the shading nets were horizontally positioned approximately 2 m above the plant canopy. The edges of the nets were secured to the ground, forming a relatively enclosed box-like shaded space to minimize the interference of external environmental factors with the shading treatment. In addition to these three inter-row artificial shading treatments, the experiment also included an under-canopy natural shading treatment (S-93, 93% natural shading). The shading treatment began at the beginning of July and ended at the end of October, as excessively high light intensity during this period is prone to have adverse effects on the growth and development of *E. pubescens*. All experimental treatments maintained consistent field management practices, including fertilization, weed control, and so on.

2.3. Measurements and Methods

2.3.1. Environmental Factor and Photosynthetic Physiological Parameters

This study was conducted during the leaf growth period (July to November). Each month, one typical sunny day was selected for in situ measurements of environmental factors (such as total radiation and vapor pressure deficit) and leaf photosynthetic characteristics (including net photosynthetic rate and stomatal conductance) using a LI6400 portable photosynthesis system (LI-COR Inc., Lincoln, NE, USA). All measurements were performed on each plot within every treatment, yielding three replicate plots per treatment. Within each plot, three leaves with consistent maturity and uniform growth direction were collected, and their values were averaged to obtain a single representative value per plot. This resulted in three replicate values per treatment (i.e., n = 3 plots per treatment) for statistical analysis. This averaging of subsamples at the plot level prior to analysis was performed to avoid pseudoreplication and ensure that the plot, rather than the individual leaf, served as the experimental unit. To characterize diurnal dynamics, measurements were

recorded hourly from 07:00 to 18:00, resulting in 12 cycles per day. From the diurnal data, we calculated the daily mean values of key environmental factors. The daily maximum net photosynthetic rate (A_n-max) and stomatal conductance (g_s-max) were determined as the average of three measurements surrounding the peak value to evaluate monthly variations in environmental conditions and leaf photosynthetic performance across different treatments. Radiation was measured using the LI-6400 built-in quantum sensor in the 400–700 nm PAR range, with data presented as daily integrated values. Vapor pressure deficit (VPD) represents the difference between the actual and saturated water vapor content in the air, indicating the degree of atmospheric dryness. An increase in VPD elevates air dryness, which induces stomatal closure to reduce transpirational water loss. This leads to a decrease in stomatal conductance and restricts CO_2 influx into leaves, ultimately inhibiting the photosynthetic rate.

2.3.2. Determination of Soil Physicochemical Properties

To assess the baseline soil conditions of the experimental site and ensure uniformity across different treatment areas, soil samples were collected in June using a "Z"-shaped sampling method. Ten representative sampling points were selected within the experimental plot, covering both under-canopy and inter-row positions. At each point, three replicate soil cores were collected from the 0–20 cm topsoil layer and mixed to form a composite sample, resulting in a total of 10 composite samples. Soil physicochemical properties—including pH, organic matter, hydrolyzable nitrogen, and available phosphorus—were determined using conventional analytical methods. The results showed no significant differences in soil physicochemical properties among sampling points, indicating that the soil conditions were homogeneous across the experimental site. The overall soil characteristics of the experimental site were as follows: pH, 6.5; organic matter, 17.96 $g \cdot kg^{-1}$; hydrolyzable nitrogen, 0.87 $g \cdot kg^{-1}$; available phosphorus, 7.61 $mg \cdot kg^{-1}$.

2.3.3. Biomass

Plant sampling was carried out monthly from July to November across all treatments. All measurements were performed on each plot within every treatment, yielding three replicate plots per treatment. For each plot, three plants exhibiting above-average growth and comparable maturity stages were selected. The biomass data from the three plants within each plot were averaged to obtain a single representative value per plot, yielding three replicate values per treatment (n = 3 plots) per month for statistical analysis. After collection, samples were immediately rinsed with distilled water and separated into leaves, stems, rhizomes, and fine roots. Each organ was placed in a separate paper envelope. They were then dried to a constant weight (mass change < 0.01 g) in a 60 °C oven (Model: GZX-9070MBE; Manufacturer: Shanghai Boxun Industrial Co., Ltd., Shanghai, China) for 48 h. The dry weight of each organ was measured using an electronic balance (Model: FA2104N; Manufacturer: Shanghai Precision Scientific Instrument Co., Ltd., Shanghai, China) with a precision of 0.01 g. Aboveground biomass is the sum of the dry weights of stems and leaves, while belowground biomass refers to the combined dry weights of roots and rhizomes.

2.3.4. Content of Medicinal Ingredients

The flavonol glycoside content was measured during the vigorous leaf growth period of *E. pubescens* (August, October, and November). To obtain plot-level data, ten uniformly growing plants were first collected from each plot and pooled to constitute one biological replicate. As each treatment consisted of three plots, a total of three biological replicates were established per treatment (i.e., n = 3 plots), resulting in 30 sampled plants in total. After drying at 60 °C, the leaf samples were ground, passed through a 50-mesh sieve, and

extracted with 50% ethanol (Thermo Fisher Scientific, Shanghai, China). The four major flavonol glycosides (epimedin A, epimedin B, epimedin C, and icariin) were quantified using an ultra-performance liquid chromatography system (Waters Corporation, ACQUITY UPLC-PDA, Milford, MA, USA) following the method of Fan et al. [36]. Total flavonol glycoside content was calculated as the sum of these four compounds. Furthermore, given the significant differences among epimedin A, B, C, and icariin in terms of their pharmacological activities, including antibacterial, antioxidant, and antitumor effects, we conducted statistical analysis of the proportions of these four medicinal components under different treatments.

2.4. Economic Benefit Analysis

To systematically evaluate the economic feasibility of *E. pubescens* cultivation under different shading treatments, economic benefit analysis was conducted based on measured per-plant biomass, actual planting density, and input costs for each treatment. To ensure comparability among treatments with different land utilization patterns, the "plot unit conversion method" was adopted to calculate the actual planting density per hectare for each treatment. This involved the following specific procedures: For understory treatments (S-0, S-50, S-75, and S-93), the planting unit consisting of four *P. zhennan* trees (2 m × 7 m) was used as the basic accounting unit. Within this unit, five ridges of *E. pubescens* were planted, with the following distribution: The natural canopy shading treatment (S-93) occupied two ridges located directly beneath the tree canopy. The inter-row shading treatments (S-0, S-50, and S-75) occupied three ridges distributed in the inter-row areas, with the same shading treatment applied within a given unit. Based on this configuration, the planting density within the unit was converted to the actual number of *E. pubescens* plants per hectare.

The economic inputs for each treatment primarily included seedling costs, land rental, and labor management expenses. Specifically, seedling costs were calculated based on actual planting density; land rental was estimated with reference to local market rates for forestland or cultivated land transfer (208.33 USD·hm^{-2}·year^{-1}); labor costs were calculated according to local wage standards and actual management frequency. Yield was expressed as aboveground dry weight (stems and leaves) per hectare (kg·hm^{-2}·year^{-1}). Economic income was calculated based on the market purchase price (22 USD·kg^{-1}), and net income was determined as total output value minus all input costs.

2.5. Statistical Analysis

Preliminary data processing, including the calculation of means and standard errors, was performed using Microsoft Excel 2019. Differences in net photosynthetic rate, biomass, and total flavonol glycoside content among treatments were assessed by one-way analysis of variance (ANOVA) in SPSS 26.0, with post hoc significance testing conducted using Duncan's multiple range test ($p < 0.05$). Bar charts, line charts, and scatter plots were generated using Origin 2021 software. A schematic diagram of the experimental site was created using Visio 2021. To explore the direct and indirect effects of environmental factors and photosynthetic parameters on biomass accumulation in *E. pubescens*, a structural equation model (SEM) was constructed using IBM SPSS Amos (version 24.0). The model was specified based on a priori theoretical assumptions: solar radiation (R) was hypothesized to indirectly regulate aboveground biomass (ABM) by modulating vapor pressure deficit (VPD) and key photosynthetic traits, including maximum net photosynthetic rate (A_n-max) and stomatal conductance (g_s-max). These pathways were informed by previous studies on plant physiological responses to light and water availability in understory environments.

Model parameters were estimated using the maximum likelihood method. The overall goodness-of-fit of the model was evaluated using multiple indices: the chi-square to degrees of freedom ratio (χ^2/df), the comparative fit index (CFI), and the root mean square error of approximation (RMSEA). Acceptable model fit was indicated by $\chi^2/df < 3.0$, CFI > 0.90, and RMSEA < 0.08, following recommended thresholds. Given the observational nature of the data, all estimated path coefficients were interpreted as statistically supported associations rather than definitive causal relationships.

3. Result

3.1. Differences in Environmental Factors Across Experimental Treatments and Their Effects on the Photosynthetic Characteristics of E. pubescens

The Vapor Pressure Deficit (VPD) under different experimental treatments gradually decreased from around 5.10 kPa in July to around 1.41 kPa in November (Figure 2A). There was no significant difference in VPD among different treatments for each month. However, the total radiation showed significant differences ($p < 0.05$) among treatments throughout the entire experimental period. The daily total radiation exhibited a gradual decline from July to November under the S-0, S-50, and S-75 treatments, whereas it remained nearly constant in the S-93. Daily total radiation exhibited the greatest divergence among treatments in July, with values of 141.30 W·m^{-2}, 93.50 W·m^{-2}, 45.59 W·m^{-2}, and 6.60 W·m^{-2} for S-0, S-50, S-75, and S-93, respectively.

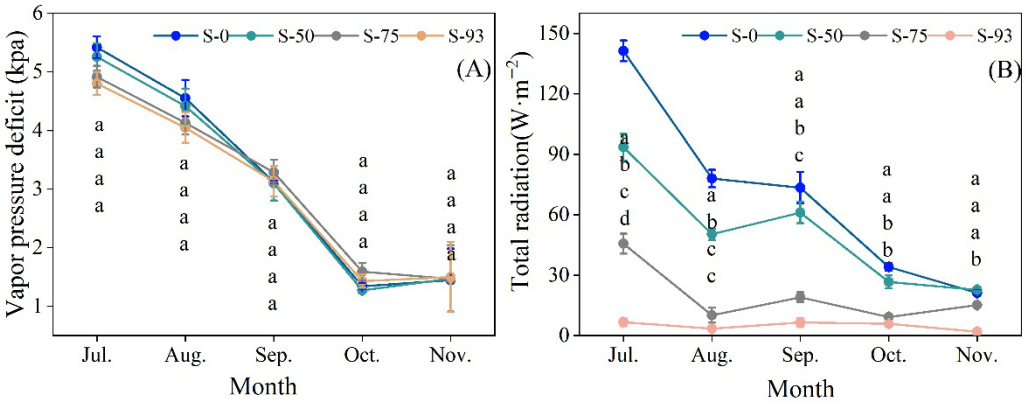


Figure 2. Monthly dynamic changes in vapor pressure deficit (VPD) and total radiation of *E. pubescens* planted under different experimental treatments (**A**) VPD monthly dynamic changes, (**B**) Total radiation monthly dynamic changes. The vertical error bars are standard deviations; different small letters at the same time indicate significant differences at the 0.05 level ($p < 0.05$). S-0, S-50, S-75 and S-93 represent 0% shading, 50% shading, 75% shading and 93% shading (under canopy), respectively.

We also analyzed the dynamic changes in A_n and g_s at different time scales and the differences between different treatments (Figures 3 and 4). We found that in August, except for A_n in S-93, the daily dynamic curve of A_n showed a trend of first increasing and then decreasing in S-0, S-50 and S-75 treatments, while the maximum value of A_n appeared later in the S-75 treatment (around 13:00) than that in the S-0 and S-50 treatments (around 12:00). In November, the A_n of S-0 still reached its maximum value around 11:00 and gradually decreased thereafter, and the A_n values of S-50 and S-75 almost reached their maxima at 10:00, continued at this level until around 13:00, and then rapidly declined. For A_n in S-93 treatment, it was almost a smooth curve with the values (0.40 μmol m^{-2} s^{-1}) during the entire experimental period. Furthermore, on a monthly scale, we found the A_n-max changed slightly with time under S-93 from July to November (Figure 4A). The A_n-max of the three inter-row treatments were almost all around 3.74 μmol m^{-2} s^{-1} in July. In August, the A_n-max values of S-0 and S-50 decreased. Conversely, the A_n-max of S-75 (3.71 μmol m^{-2} s^{-1})

remained unchanged and was significantly higher than that of S-0 (2.15 μmol m^{-2} s^{-1}) or S-50 (2.49 μmol m^{-2} s^{-1}) ($p < 0.05$). Afterwards, the significant increase in A_n-max of S-0 and S-50 reached (4.66 μmol m^{-2} s^{-1} and 4.58 μmol m^{-2} s^{-1}) in November. In addition, from July to November, compared to S-93 treatment, the A_n-max of S-0, S-50, and S-75 treatments significantly increased by 30%–50%, 50%–70%, and 40%–80%, respectively.

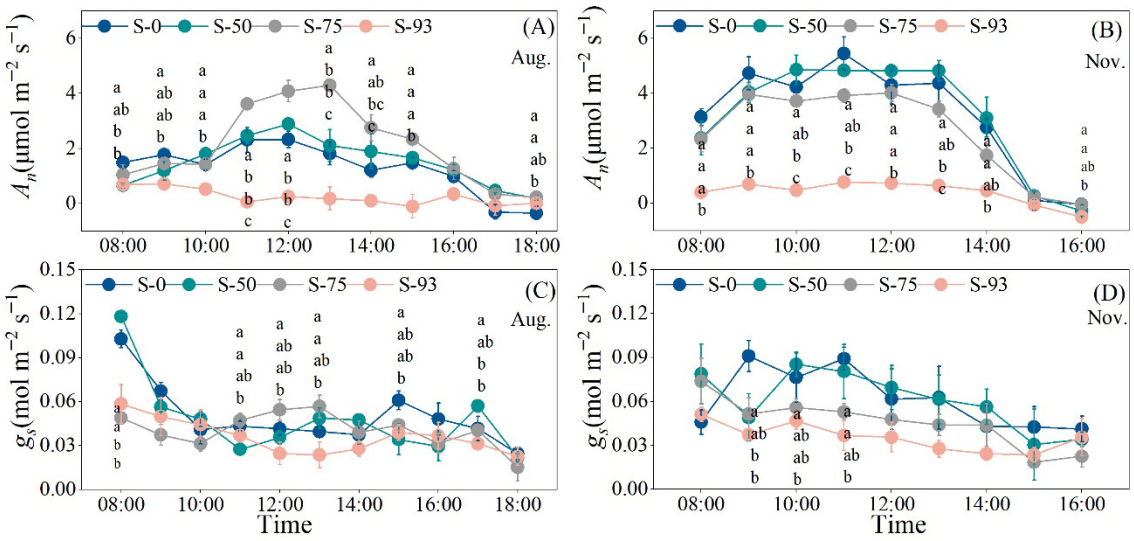


Figure 3. The daily dynamic changes in photosynthetic indicators of *E.pubescens* planted under different experimental treatments in August and November. (**A**,**B**) Net photosynthetic rate daily dynamic changes; (**C**,**D**) stomatal conductance daily dynamic changes. The vertical error bars are standard deviations; different small letters at the same time indicate significant differences at the 0.05 level ($p < 0.05$). S-0, S-50, S-75 and S-93 represent 0% shading, 50% shading, 75% shading and 93% shading (under canopy), respectively. A_n: net photosynthetic rate; g_s: stomatal conductance.

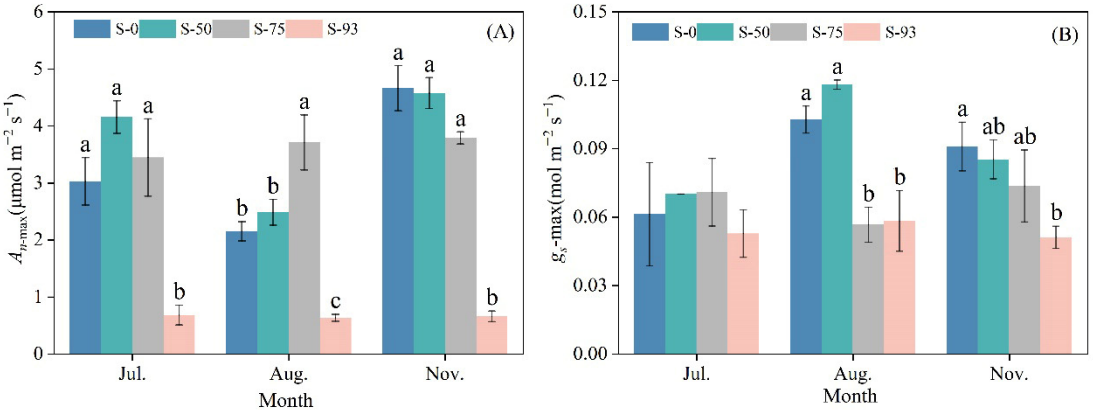


Figure 4. Monthly dynamics of photosynthetic parameters in *E. pubescens* under different experimental treatments (July, August, and November). (**A**) Net photosynthetic rate monthly dynamic changes; (**B**) stomatal conductance monthly dynamic changes. The vertical error bars are standard deviations; different small letters at the same time indicate significant differences at the 0.05 level ($p < 0.05$). S-0, S-50, S-75 and S-93 represent 0% shading, 50% shading, 75% shading and 93% shading (under canopy), respectively. A_n-max: maximum net photosynthetic rate; g_s-max: maximum stomatal conductance.

The daily dynamic trend of g_s showed different trends in different months (Figure 3C,D). In August, the daily dynamics of g_s in S-0 and S-50 treatments rapidly decreased from 8:00 am (0.10~0.12 mol m^{-2} s^{-1}) to 10:00 am (0.04~0.05 mol m^{-2} s^{-1}), with little change thereafter. However, the daily dynamics of g_s at S-75 and S-93 treatments showed relatively mild changes, with the maximum values occurring around 13:00 (0.06 mol m^{-2} s^{-1}) and

8:00 (0.06 mol m^{-2} s^{-1}), respectively. In November, the daily dynamic curves of g_s for all experimental treatments fluctuated around 0.08 mol m^{-2} s^{-1}. Furthermore, on a monthly scale, we found that the g_s -max in S-93 treatment showed almost no significant fluctuations from July to November (Figure 4B). The g_s -max values in S-0, S-50, and S-75 treatments showed varying degrees of fluctuation from July to November, and reached their maximum values in August, August, and November, respectively. In addition, in August, g_s -max was significantly higher in S-0 and S-50 treatments than in S-75 and S-93 treatments ($p < 0.01$). In October, g_s -max in S-50 was significantly higher than in the other three experimental treatments ($p < 0.01$), with values of 0.11, 0.34, 0.08, and 0.07 mol m^{-2} s^{-1} in S-0, S-50, S-75, and S-93 treatments, respectively.

3.2. Characteristics of Biomass and Total Flavonoid Glycosides Changes of E. pubescens Under Different Experimental Treatments

In this study, we investigated the dynamic changes in the aboveground and belowground biomass of *E. pubescens* in four experimental treatments planted under the Nanmu trees (Figure 5). In August, one month after the shading treatment in Nanmu-*E. pubescens* intercropping system, we found that the aboveground biomass of *E. pubescens* under S-75 and S-50 treatments was significantly higher than that under the S-93 treatment ($p < 0.05$). However, the underground biomass of the S-50 treatment was significantly higher than those of S-75 and S-93 ($p < 0.01$). In October, the aboveground biomass of the three experimental treatments in tree rows (S-0, S-50, S-75) was much higher than that of the S-93, with the values 32.02~36.72 g/plant and 11.97 g/plant in three inter-row experimental treatments and S-93, respectively. Interestingly, the underground biomass also showed the same trend as aboveground biomass among four intercropping treatments (Figure 5B). In November (the harvest period), the differences in biomass among treatments became more pronounced. The aboveground biomass of the S-75 treatment (42.22 ± 4.04 g/plant) was significantly higher than that of the S-0 (33.76 ± 2.26 g/plant), S-50 (32.18 ± 1.08 g/plant), and S-93 (12.18 ± 0.89 g/plant) treatments. Regarding belowground biomass, the values of the S-0, S-50, and S-75 treatments (ranging from 20.50 ± 2.24 to 25.01 ± 1.69 g/plant) were all significantly higher than that of the S-93 treatment (6.31 ± 1.73 g/plant).

The total flavonol glycosides were measured in all treatments in August, October, and November (Figure 6). We found that there was no significant difference in the total flavonoid glycoside content among all treatments during the entire experimental period, with the values of 3.63~4.04%, 3.27~4.11%, and 6.05~7.01% obtained in August, October, and November, respectively. Obviously, the total flavonoid glycoside content of *E. pubescens* was dominated by icariin (Table A1), with proportions of 64.47~68.50%, 56.26~62.93%, and 47.78~53.96% in August, October, and November, respectively. Compositional analysis of the four components showed: In August, the epimedin A content in *E. pubescens* under the S-50 treatment was significantly higher than that under the S-0 and S-75 treatments ($p < 0.05$), while no significant differences were observed among treatments for the other medicinal components. In October, the epimedin C content under the S-93 treatment was significantly higher than that under the three shading treatments ($p < 0.05$). Regarding icariin, the S-0 treatment exhibited the highest content in both October and November, with values of 62.93 ± 0.56% and 53.96 ± 0.85%, respectively.

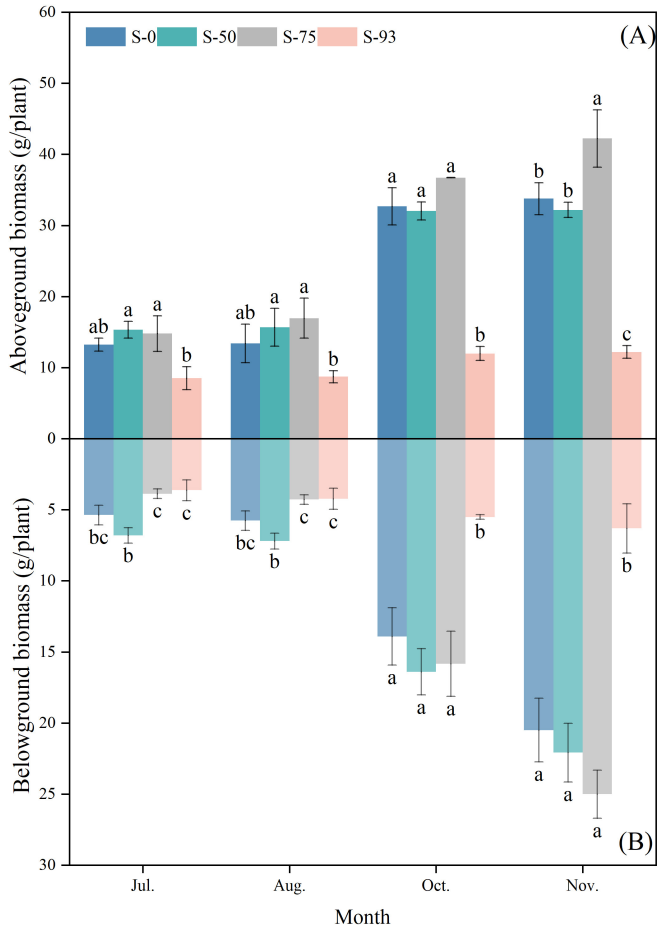


Figure 5. Changes in biomass during August, October and November. (**A**) Changes in aboveground biomass (aboveground: stems, leaves). (**B**) Changes in underground biomass (subsurface: roots, rhizomes). The vertical error bars are standard deviations; different small letters at the same time indicate significant differences at the 0.05 level ($p < 0.05$). S-0, S-50, S-75, and S-93 represent 0% shading, 50% shading, 75% shading, and 93% shading (under canopy), respectively.

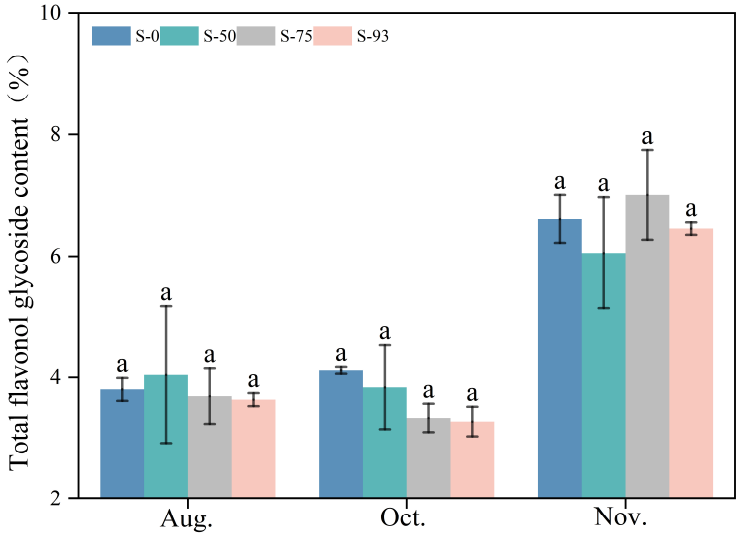


Figure 6. During August, October and November, the total flavonol glycoside content of different experimental treatments are measured each month. The vertical error bars are standard deviations; different small letters at the same time indicate significant differences at the 0.05 level ($p < 0.05$). S-0, S-50, S-75, and S-93 represent 0% shading, 50% shading, 75% shading, and 93% shading (under canopy), respectively.

3.3. Pathway Analysis of Environmental and Physiological Factors Underlying Biomass Formation of E. pubescens

While the monthly mean VPD did not differ significantly among treatments (Figure 2A), driven by fluctuations in radiation, it may still exert a regulatory role on plant physiology. To explore this underlying mechanism, we employed structural equation modeling (χ^2/df = 0.60, CFI = 1.00, RMSEA = 0) to disentangle the interactive effects of environmental and physiological factors on biomass accumulation (Figure 7). The results demonstrated that the environmental factor VPD exerted significant negative effects on both leaf physiological parameters g_s-max ($\beta = -0.53$) and A_n-max ($\beta = -0.58$), while also showing a significant negative influence on aboveground biomass (ABM) ($\beta = -0.58$). The environmental factor R exhibited significant positive effects on both atmospheric VPD ($\beta = 0.56$) and A_n-max ($\beta = 0.70$), but showed no significant relationships with g_s-max, ABM, or underground biomass (UBM). Furthermore, A_n-max displayed a significant positive effect on ABM ($\beta = 0.46$), but no significant association with UBM was observed.

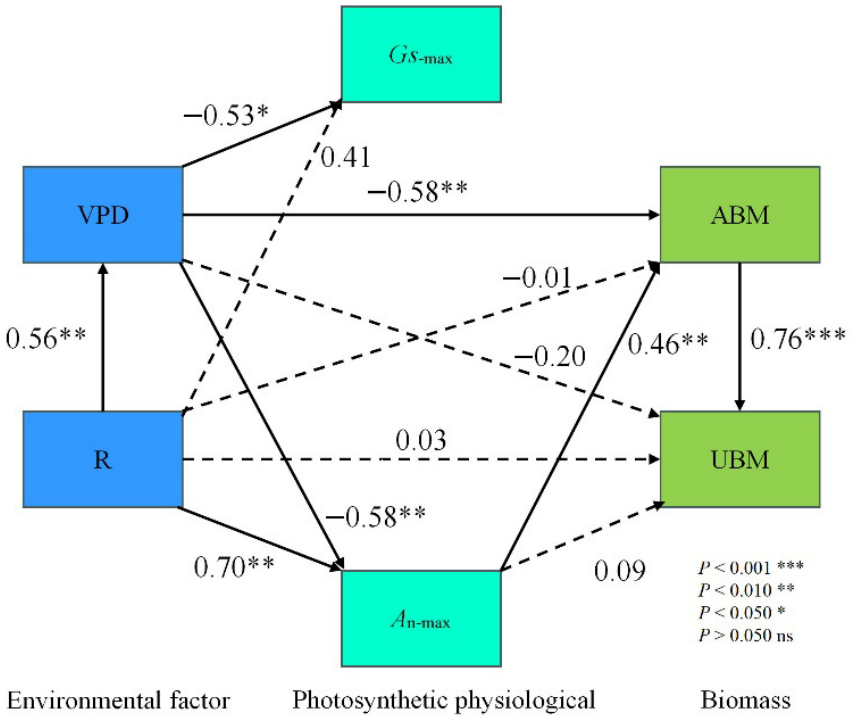


Figure 7. Assessing causal pathways: a structural equation model linking environmental factors, physiological factors, and biomass accumulation. Standardized path coefficients (ρ: −1 to 1) are indicated along path arrows, where positive and negative values represent positive and negative effects, respectively. Asterisks represent significance levels ($p < 0.001$, ***; $p < 0.010$, **; $p < 0.05$, *; $p > 0.05$, ns). R: total radiation; VPD: vapor pressure deficit; g_s-max: maximum stomatal conductance; A_n-max: maximum net photosynthetic rate; ABM: aboveground biomass; UBM: underground biomass.

The relationship between aboveground biomass and A_n-max has also been explored. We found that aboveground biomass could be quantitatively described by A_n-max through a logarithmic relationship ($R^2 = 0.95$, $p < 0.001$) (Figure 8). However, there was no significant relationship between the underground biomass and A_n-max. Additionally, there was no significant relationship between the content of total flavonoid glycosides and A_n-max.

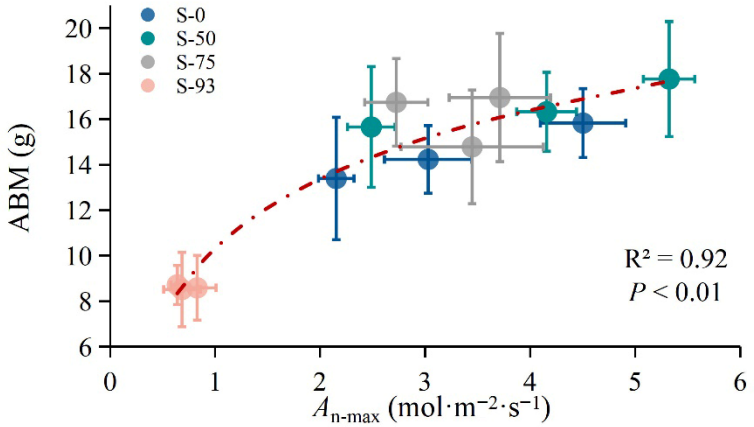


Figure 8. Correlation analysis between aboveground biomass and A_n-max. The vertical error bars are standard deviations. S-0, S-50, S-75 and S-93 represent 0% shading, 50% shading, 75% shading and 93% shading (under canopy), respectively. ABM: aboveground biomass; A_n-max: maximum net photosynthetic rate.

3.4. Economic Income of E.pubescens Planted Under Different Experimental Treatments

The results of the economic analysis indicated that the S-93 treatment achieved the lowest yield. Furthermore, the adoption of understory management practices comparable to the S-75 treatment in this study could generate a net income of 56,924.5 USD·hm^{-2}·year^{-1} after deducting various costs (including seedlings, land rental, and labor) (Table A2).

4. Discussion

Compared to the uniform shading conditions in conventional field cultivation, the understory planting of medicinal plants faces challenges such as significant environmental gradients and unclear cultivation management practices, which hinder the guarantee of yield and quality. Previous studies have indicated that understory environmental factors (light, temperature, water) interact in complex nonlinear ways, collectively regulating the photosynthetic physiological functions of understory crops, thereby ultimately determining their growth dynamics and quality [37]. Empirical evidence from systems such as jujube tree–wheat and broad-leaved forest–*Sarcandra glabra* recorded understory light transmittance as low as 30%–50%, substantially lower than in conventional monoculture [38,39]. Consequently, this light reduction drives microclimatic changes, including lower air temperatures and higher relative humidity, as documented in the understory cultivation of *Polygonatum kingianum* and *Flemingia philippinensis* [3,40], confirming light is the principal factor governing micro-environment formation. Given that photosynthesis underpins biomass and yield, the synergistic influence of these environmental factors is critically important [41]. For example, shading intensity values in jujube–wheat, apricot–wheat, and walnut–wheat systems reached 23.2%, 57.5%, and 80.7%, respectively, correlating with photosynthetic rate reductions of 11.3%, 31.9%, and 36.2% compared to monoculture wheat [42]. Nonetheless, research has predominantly focused on the implications of natural shading, overlooking the potential photoinhibitory stress that high-light conditions in forest gaps or edges may impose on shade-preferring species. Furthermore, while studies on crops like peanut, wheat, corn, and *Liriope spicata* have demonstrated that understory spatial heterogeneity significantly affects yield and quality [43–45], the systematic evaluation of medicinal plants across different understory locations is lacking, hindering the development of standardized cultivation protocols.

This study demonstrates that heterogeneity in the understory light environment significantly affects the growth and physiological responses of *E. pubescens*. Aboveground biomass showed an increasing trend as shading intensity rose from 0% to 75%, whereas

severe shading under the natural forest canopy (S-93) severely inhibited photosynthesis and biomass accumulation. This finding is consistent with Zhang et al. [33], who reported that *E. pubescens* performs optimally under moderate to low light intensities and is inhibited under both excessively high- and low-light conditions, further confirming the shade-preferring characteristics of this species and its dependence on light availability. This validates our first hypothesis.

Regarding the effects of light on secondary metabolism in medicinal plants, this study found no significant differences in total flavonol glycoside content among treatments. This result appears to diverge from some previous studies. For example, Wang et al. [46] reported that 60% light transmittance significantly promoted the accumulation of specific flavonoids in Alpinia katsumadai, while Wu et al. [47] identified an optimal light transmittance range of 10%–25% for saponin accumulation in *Panax notoginseng*. We propose that these discrepancies may arise from the following factors. The first is a species-specific response: different medicinal plants possess fundamentally different adaptive strategies and secondary metabolic regulatory pathways in response to light. The second is heterogeneity in experimental conditions: previous studies were mostly conducted under controlled pot conditions with single environmental factors, which cannot fully replicate the synergistic interactions of light, temperature, and humidity under forest understory conditions. The third is differences in the granularity of observational indices: although total flavonol glycoside content showed no significant changes in this study, the possibility of adaptive adjustments in the proportions of individual compounds cannot be excluded, and such compositional shifts may have potential biological or pharmacological significance worthy of further investigation.

Notably, although the monthly mean vapor pressure deficit showed no significant differences among shading treatments, structural equation modeling revealed its indirect regulatory role in photosynthetic physiology and biomass accumulation through temporal variation. We propose a potential regulatory pathway of "solar radiation–vapor pressure deficit–photosynthetic rate–aboveground biomass." However, we acknowledge that while SEM can reveal the strength of associations among variables, the data from this study are insufficient to fully confirm the underlying physiological mechanisms. For example, how photosynthates are specifically allocated to different metabolic pathways, and whether this allocation is influenced by interactions between light intensity and soil nutrients or water, requires further validation. Therefore, we consider this pathway as a working model to be tested in future research.

Future studies should prioritize the following steps: First, it is necessary to integrate the monitoring of plant–soil water and nutrient dynamics to comprehensively disentangle the direct and indirect effects of shading in agroforestry systems. Second, we must conduct multi-site, multi-year trials to validate the generalizability of our findings. Third, we must develop a coupled "light–photosynthesis–yield/quality" predictive model that fully accounts for species specificity, light quality effects, developmental stage differences, and consistency in metabolite detection methods. This will ultimately contribute to a comprehensive understanding of understory light regulation mechanisms and provide a solid theoretical basis for developing precision cultivation management strategies for *E. pubescens* and other shade-tolerant medicinal plants.

5. Conclusions

This study demonstrates that shading intensity was a critical environmental factor governing the growth and economic viability of *E. pubescens* cultivated in *P. zhennan*-based agroforestry systems. We identified 75% shading as the optimal level for cultivating *E. pubescens* under *P. zhennan* plantations, which promoted the accumulation of both biomass

and medicinal quality while delivering the greatest economic return. Based on our single-site, one-year field experiment, we identified 75% shading as a potentially optimal level for cultivating *E. pubescens* under *P. zhennan* plantations in this specific context, as it promoted the accumulation of both biomass and medicinal quality while delivering the greatest economic return. In contrast, 93% shading under the tree canopy significantly suppressed photosynthetic capacity and biomass accumulation. The application of structural equation modeling elucidated the underlying mechanism: light intensity indirectly influences yield by synergistically regulating vapor pressure deficit and net photosynthetic rates. These findings provide a scientific basis for optimizing light management in the understory cultivation of *E. pubescens*. The methodology and insights gained, particularly the quantitative relationship between light environment and plant performance, may offer a valuable reference framework for studying other high-value, shade-tolerant medicinal plants; however, the direct applicability of our specific findings to other species remains a hypothesis requiring further validation. This contributes to alleviating the conflict between land scarcity and the growing demand for herbal resources. Future research should focus on first validating these optimal thresholds as site- and season-specific findings through multi-site, multi-year trials across different tree species, geographical locations, and seasonal cycles. Further investigation is also warranted to explore the long-term dynamics of soil health and plant quality within this specific agroforestry system.

Author Contributions: D.L.: Project administration, Validation, Writing—review and editing. H.Z.: Data curation, Formal analysis, Visualization, Writing—original draft. D.W.: Investigation, Data curation, Software. F.S.: Resources. B.G.: Funding acquisition, Methodology, Resources, Supervision. All authors have read and agreed to the published version of the manuscript.

Funding: The authors declare financial support was received for the research and/or publication of this article. This research was jointly financially supported by the National Key Research and Development Program of China (Grant No. 2025YFC3509201) and the CAMS Innovation Fund for Medical Sciences (CIFMS) (2021-I2M-1-031).

Data Availability Statement: The original contributions presented in the study are included in the article. Further inquiries can be directed to the corresponding author.

Acknowledgments: Thanks to Shawan District *E. pubescens* Industrial Park for providing experimental materials for the research.

Conflicts of Interest: The authors declare no conflicts of interest.

Appendix A

Table A1. Multiple Comparison Analysis of four medicinal components of *E. pubescens* among treatments from August to November. The different lowercase letters in table indicate significant differences ($p < 0.05$). S-0: No shading net; S-50: 50% shading between rows in the *P. zhennan* forest; S-75: 75% shading between rows in the *P. zhennan* forest; S-93: 93% shading under the *P. zhennan* tree canopy; CK: Conventional field cultivation.

Treatment		Epimedin A (%)	Epimedin B (%)	Epimedin C (%)	Icariin (%)
August	S-0	12.52 ± 0.46 c	10.69 ± 0.61 b	10.43 ± 0.36 a	66.36 ± 1.28 a
	S-50	14.34 ± 0.34 b	10.72 ± 0.77 b	9.72 ± 0.82 a	68.50 ± 4.83 a
	S-75	12.59 ± 0.75 c	10.76 ± 0.71 b	10.56 ± 0.73 a	66.08 ± 1.98 a
	S-93	12.74 ± 0.35 bc	11.03 ± 0.58 b	11.75 ± 0.29 a	64.47 ± 0.63 a
October	S-0	13.52 ± 0.04 a	11.87 ± 0.17 a	11.68 ± 0.72 b	62.93 ± 0.56 a
	S-50	13.10 ± 0.88 a	11.60 ± 0.96 a	13.35 ± 1.07 b	61.96 ± 2.02 bc
	S-75	13.92 ± 0.71 a	12.73 ± 0.69 a	11.95 ± 0.57 b	61.40 ± 1.95 bc
	S-93	14.14 ± 0.56 a	12.47 ± 0.36 a	17.14 ± 1.52 a	56.26 ± 1.67 b
November	S-0	8.14 ± 0.16 a	14.28 ± 0.56 a	23.62 ± 0.47 a	53.96 ± 0.85 a
	S-50	9.09 ± 0.33 a	15.61 ± 1.32 a	27.52 ± 1.29 a	47.78 ± 0.51 b
	S-75	9.05 ± 0.60 a	15.74 ± 0.39 a	22.79 ± 1.03 a	52.42 ± 0.96 ab
	S-93	9.24 ± 0.59 a	15.51 ± 0.93 a	26.29 ± 2.88 a	48.96 ± 2.43 ab

Table A2. Input cost, plant yield and economic income of *E. pubescens* cultivated in different location under *P. zhennan* trees. S-0: No shading net; S-50: 50% shading between rows in the *P. zhennan* forest; S-75: 75% shading between rows in the *P. zhennan* forest; S-93: 93% shading under the *P. zhennan* tree canopy; CK: Conventional field cultivation.

Treatment	Number of Plants	Seedling Costs	Land Rental Costs	Labor Management Costs	Dry Weight of Stem and Leaf	Unit Price	Total Income	Net Income
	(plant·hm^{-2})	(USD·hm^{-2})	(USD·hm^{-2})	(USD·hm^{-2}·year^{-1})	(kg·hm^{-2})	(USD·kg^{-1})	(USD·hm^{-2})	(USD·hm^{-2})
S-0	85,725	18,585	125	3984	2886	22	63,492	40,799
S-50	85,725	18,585	125	3984	2759	22	60,698	38,005
S-75	85,725	18,585	125	3984	3619	22	79,618	56,925
S-93	57,150	12,392	83	2657	696	22	15,312	180

References

1. Qiao, X.; Sai, L.; Chen, X.; Xue, L.; Lei, J. Impact of fruit-tree shade intensity on the growth, yield, and quality of intercropped wheat. *PLoS ONE* **2019**, *14*, e0203238. [CrossRef]
2. Zhang, W.; Liu, C.R.; Zhou, Y.M.; Zhou, H.; Xie, H. Correlation between tree structure, light environment and wheat yield in almond-winter wheat intercropping pattern. *Xinjiang Agric. Sci.* **2019**, *56*, 2238–2246.
3. Xiao, L.J.; Wu, J.L.; Xiao, J.X. Effects of environmental factors under walnut forest on photosynthesis, yield and quality of *Polygonatum kingianum*. *J. Northwest For. Univ.* **2024**, *39*, 108–116.
4. Chang, X.W.; Ling, Q.; Gao, H. Effects of different planting patterns on the quality and yield of *Polygonatum cyrtonema*. *J. Yunnan Agric. Univ. (Nat. Sci.)* **2025**, *40*, 108–116.
5. Li, F.; Meng, P.; Fu, D.; Wang, B. Light distribution, photosynthetic rate and yield in a Paulownia-wheat intercropping system in China. *Agrofor. Syst.* **2008**, *74*, 163–172. [CrossRef]
6. Zhao, Y.; Qiao, J.; Wang, W.W.; Wang, B.P.; Zhou, H.H.; Cui, L.J.; Duan, W.; Su, L.Y. Response of wheat yield to photosynthetically active radiation distribution within paulownia shelterbelt system. *Chin. J. Eco-Agric.* **2017**, *25*, 647–655.
7. Xiao, J.H.; Ding, X.; Li, L.; Ma, H.; Ci, X.Q.; van der Merwe, M.; Li, J.; Conran, J.G. Miocene diversification of a golden-thread nanmu tree species (*Phoebe zhennan*, Lauraceae) around the Sichuan Basin shaped by the east Asian monsoon. *Ecol. Evol.* **2020**, *10*, 10543–10557. [CrossRef] [PubMed]
8. Yang, H.; An, W.; Gu, Y.; Peng, J.; Jiang, Y.; Li, J.; Wan, X.; Chen, L.; Zhu, P.; He, F.; et al. Integrative metabolomic and transcriptomic analysis reveals the mechanism of specific color formation in *Phoebe zhennan* heartwood. *Int. J. Mol. Sci.* **2022**, *23*, 13569. [CrossRef] [PubMed]
9. Yang, H.; Huang, X.; Gu, Y.; Peng, J.; Luo, X.; Zhang, S.; Guo, H.; Jiang, Y.; Xie, J.; Liu, M.; et al. Influence of tree age on the wood color and compounds involved in the golden-thread wood color formation in *Phoebe zhennan*. *Ind. Crop. Prod.* **2024**, *221*, 119406. [CrossRef]
10. Yang, H.; Zhang, S.; Gu, Y.; Peng, J.; Huang, X.; Guo, H.; Wan, X.; Jiang, Y.; Xie, J.; Liu, M.; et al. Identification and variation analysis of the composition and content of essential oil and fragrance compounds in *Phoebe zhennan* wood at different tree ages. *Front. Plant Sci.* **2024**, *15*, 1368894. [CrossRef]
11. Hsieh, T.P.; Sheu, S.Y.; Sun, J.S.; Chen, M.H.; Liu, M.H. Icariin isolated from *Epimedium pubescens* regulates osteoblasts anabolism through BMP-2, SMAD4, and Cbfa1 expression. *Phytomedicine* **2010**, *17*, 414–423. [CrossRef]
12. Qin, Z.; Liao, D.; Chen, Y.; Zhang, C.; An, R.; Zeng, Q.; Li, X. A widely metabolomic analysis revealed metabolic alterations of *Epimedium pubescens* leaves at different growth stages. *Molecules* **2019**, *25*, 137. [CrossRef] [PubMed]
13. Cheng, Q.; Yang, S.; Li, S.; Xiao, M.; Yang, J.; Li, Y.; Cheng, C. Prioritization of Germplasm Resources for Epimedium Breeding: Chemotype Oriented Discovery Using Cross Latitude Scale Resource Evaluation. *Ind. Crop. Prod.* **2025**, *238*, 122365. [CrossRef]
14. Feng, Y.F.; Zheng, R.L.; Tang, Z.K.; Chen, P.; Zhang, D.Q.; Yuan, X.H. Screening of strains for transformation of flavonoids from *Epimedium pubescens* and their biotransformation effect on caohuoside C. *Microbiol. China* **2025**, *53*, 1–23. [CrossRef]
15. Zhang, H.B.; Wen, D.M.; Qin, F.Y.; Suo, F.M.; Li, D.D.; Guo, B.L. Effects of understory environmental factors on the yield and content dynamic changes of *Epimedium pubescens*. *China J. Chin. Mater. Med.* **2025**, *50*, 6309–6318. [CrossRef]
16. Qiao, X.; Xiao, L.; Gao, Y.; Zhang, W.; Chen, X.; Sai, L.; Li, A.; Lei, J.; Xue, L.; Zhang, Y. Yield and quality of intercropped wheat in jujube- and walnut- based agroforestry systems in southern Xinjiang Province, China. *Agron. J.* **2020**, *112*, 2676–2691. [CrossRef]
17. Feng, B.; Xu, G.H.; Liu, J.Y.; Li, C.L. Effects of different light intensities on matter accumulation and yield of *Allium victorialis* under forest imitation cultivation in Changbai Mountain area. *J. Shandong Agric. Univ. (Nat. Sci. Ed.)* **2023**, *54*, 65–70.
18. Yang, B.; Gong, P.; Che, Y.H.; Zhang, P.; Xu, Y.; Yang, L. Study on almond and cotton intercropping to yield of cotton. *Chin. Agric. Sci. Bull.* **2009**, *25*, 93–97.

19. Shang, S.J.; Wang, Y.J.; Wang, N.; Yang, J.L.; Xu, S.; He, X.Y.; Chen, W. Effects of light intensity on physiological and growth characteristics of *Paeonia rockii*. *Chin. J. Ecol.* **2020**, *39*, 2963.
20. Gao, Q.M.; Ren, L.H.; Mi, Z.R.; Meng, Q.F.; Dong, Q.Y.; Han, J.L.; Wang, Z.F. Effects of different light intensities on the growth and photosynthetic characteristics of *Polygonatum cyrtonema*. *Shandong Agric. Sci.* **2021**, *53*, 44.
21. Zheng, D.H.; Yuan, S.N.; Chen, J.M.; Huang, J.X.; Pan, J.; Li, J.; Zhou, L.J. Study on yield and medicinal material quality of *Desmodium styracifolium* intercropped in rubber forest. *J. Chin. Med. Mater.* **2017**, *40*, 2765–2771.
22. Zheng, D.H.; Huang, J.X.; Pan, J.; Yuan, S.N.; Gui, Q.; Li, J.; Wang, X.Q. Study on growth, yield and medicinal quality of *Gynostemma pentaphyllum* intercropped in rubber plantations with different canopy densities. *J. Chin. Med. Mater.* **2021**, *44*, 1058–1064.
23. Roces-Díaz, J.V.; Vayreda, J.; De Cáceres, M.; García-Valdés, R.; Banqué-Casanovas, M.; Morán-Ordóñez, A.; Brotons, L.; de-Miguel, S.; Martínez-Vilalta, J. Temporal changes in Mediterranean forest ecosystem services are driven by stand development, rather than by climate-related disturbances. *For. Ecol. Manag.* **2021**, *480*, 118623. [CrossRef]
24. Xu, Z.F.; Liu, C.S.; Liao, X.D.; Sui, J.H.; Chen, Y.Q.; Chen, C.B.; Wei, L.N. Effects of ecological factors on the quality difference between forest land *ginseng* and farmland ginseng. *J. Agric. Sci. Technol.* **2024**, *26*, 213–223.
25. Long, S.P.; Zhu, X.G.; Naidu, S.L.; Ort, D.R. Can improvement in photosynthesis increase crop yields? *Plant Cell Environ.* **2006**, *29*, 315–330. [CrossRef] [PubMed]
26. Zhu, X.G.; Long, S.P.; Ort, D.R. Improving photosynthetic efficiency for greater yield. *Annu. Rev. Plant Biol.* **2010**, *61*, 235–261. [CrossRef]
27. Qu, M.; Zheng, G.; Hamdani, S.; Essemine, J.; Song, Q.; Wang, H.; Chu, C.; Sirault, X.; Zhu, X.G. Leaf photosynthetic parameters related to biomass accumulation in a global rice diversity survey. *Plant Physiol.* **2017**, *175*, 248–258. [CrossRef]
28. Kaiser, E.; Morales, A.; Harbinson, J.; Kromdijk, J.; Heuvelink, E.; Marcelis, L.F. Dynamic photosynthesis in different environmental conditions. *J. Exp. Bot.* **2015**, *66*, 2415–2426. [CrossRef]
29. Zheng, H.; Zheng, L.; Yu, X. Non-Targeted Metabolomics Study of *Epimedium pubescens* in Response to Light Stress. *J. Plant Growth Regul.* **2025**, *44*, 5682–5691. [CrossRef]
30. Li, P.; Xiang, Q.; Wang, Y.; Dong, X. UV-B Radiation Enhances *Epimedium brevicornu* Maxim. Quality by Improving the Leaf Structure and Increasing the Icaritin Content. *Plants* **2024**, *13*, 1720. [CrossRef] [PubMed]
31. Jiang, Z.; Jia, Z.; Zhang, J.; Chen, H.; Duan, H.; Zhao, W. Effects of light quality on growth and accumulation of active components in Epimedium. *Chin. Tradit. Herb. Drugs* **2025**, 2421–2426.
32. Ma, W.Q.; Xu, C.Q.; Guo, B.L.; Zhang, L.J. Effects of different light intensities on growth characteristics and icariin ketoside content of *Epimedium pubescens*. *Mod. Chin. Med.* **2023**, *25*, 847–853.
33. Dai, A.; Zhang, Y.; Ai, Q.; Teng, X.; Yang, L. Effects of different light qualities on growth, physiology and flavonoids accumulation of *Epimedium koreanum* Nakai. *J. Agric. Sci. Technol.* **2022**, *24*, 85–92.
34. He, L.; Chen, L.; Li, Y.; Fu, R.; Quan, Q.; Gao, H. Photosynthetic characteristics and environmental adaptability analysis of *Epimedium pubescens* Maxim. *J. Anhui Agric. Sci.* **2016**, *44*, 1–3+6.
35. Wang, Y.; Mao, X.Y.; Ding, Y.; Yu, H.X.; Ran, Z.F.; Chen, X.L.; Zhou, J. Differences in growth and secondary metabolite accumulation of *Panax quinquefolius* cultivated under forest and in field in Shandong. *China J. Chin. Mater. Med.* **2025**, *50*, 1524–1533.
36. Fan, X.L.; Xu, C.Q.; Cao, Y.; Guo, B.L.; Luo, G.M. Correlation between ecological factors and the content of pharmacodynamic components and flower and leaf traits of *Epimedium pubescens*. *China J. Chin. Mater. Med.* **2024**, *49*, 3194–3203.
37. Rigal, C.; Xu, J.; Hu, G.; Qiu, M.; Vaast, P. Coffee production during the transition period from monoculture to agroforestry systems in near optimal growing conditions, in Yunnan Province. *Agric. Syst.* **2020**, *177*, 102696. [CrossRef]
38. Zhang, W.; Wang, B.J.; Gan, Y.W.; Duan, Z.P.; Hao, X.D.; Xu, W.L.; Li, L.H. Different tree age affects light competition and yield in wheat grown as a companion crop in jujube-wheat agroforestry. *Agrofor. Syst.* **2019**, *93*, 653–664. [CrossRef]
39. Mo, L.; Jiang, Q.W.; Feng, J.J.; Liao, J.X. Effects of broad-leaved forest and full-light cultivation on photosynthetic characteristics of *Sarcandra glabra*. *Mod. Hortic.* **2023**, *46*, 7.
40. Zuo, J.L.; Zhou, W.C.; Huang, J.J.; Chen, Z.; Lu, X. Study on the effects of intercropping medicine in young *Camellia oleifera* forest on stand temperature and light. *Acta Agric. Jiangxi* **2022**, *34*, 56.
41. van Rooijen, R.; Aarts, M.G.; Harbinson, J. Natural genetic variation for acclimation of photosynthetic light use efficiency to growth irradiance in *Arabidopsis*. *Plant Physiol.* **2015**, *167*, 1412–1429. [CrossRef]
42. Xu, Z.; Jiang, Y.; Zhou, G. Response and adaptation of photosynthesis, respiration, and antioxidant systems to elevated CO_2 with environmental stress in plants. *Front. Plant Sci.* **2015**, *6*, 701. [CrossRef]
43. Bai, W.; Sun, Z.; Zheng, J.; Du, G.; Feng, L.; Cai, Q.; Yang, N.; Feng, C.; Zhang, Z.; Evers, J.; et al. Mixing trees and crops increases land and water use efficiencies in a semi-arid area. *Agric. Water Manag.* **2016**, *178*, 281–290. [CrossRef]
44. Qiao, X.; Chen, X.; Lei, J.; Sai, L.; Xue, L. Apricot-based agroforestry system in Southern Xinjiang Province of China: Influence on yield and quality of intercropping wheat. *Agrofor. Syst.* **2020**, *94*, 477–485. [CrossRef]

45. Zhang, J.J.; Wan, X.; Wang, B.S.; Wang, L.; Xing, W. Analysis of growth status of *Liriope spicata* and soil properties in forest land under interplanting with different tree species. *J. South. Agric.* **2023**, *54*, 2901–2909.
46. Wang, X.B.; Han, Q.; Lin, M.P.; Li, K.L.; Pan, D.K.; Zhao, W.W.; Zhou, S.P. Effects of light conditions on microclimate and the growth and quality of *Alpinia katsumadai* in forest-medicinal plant intercropping. *J. Cent. South Univ. Technol.* **2024**, *44*, 55–61.
47. Wu, C.; Ye, C.; Zhang, J.X.; Gong, J.S.; Li, T.Y.; Yang, M.; Zhu, S.S. Effects of habitat differences under Pinus kesiya forest on growth and quality of *Panax notoginseng*. *J. Yunnan Agric. Univ. (Nat. Sci.)* **2021**, *36*, 691–699.

Disclaimer/Publisher's Note: The statements, opinions and data contained in all publications are solely those of the individual author(s) and contributor(s) and not of MDPI and/or the editor(s). MDPI and/or the editor(s) disclaim responsibility for any injury to people or property resulting from any ideas, methods, instructions or products referred to in the content.